MOLECULAR AND CELLULAR BIOLOGY, Jan. 2005, p. 206–219 Vol. 25, No. 1
0270-7306/05/$08.00+0 doi:10.1128/MCB.25.1.206–219.2005
Copyright © 2005, American Society for Microbiology. All Rights Reserved.

Core Promoter Binding by Histone-Like TAF Complexes

Hanshuang Shao,[1]†‡ Merav Revach,[1]† Sandra Moshonov,[1] Yael Tzuman,[1] Kfir Gazit,[1] Shira Albeck,[2] Tamar Unger,[2] and Rivka Dikstein[1]*

Department of Biological Chemistry[1] and Israel Structural Proteomic Center,[2] The Weizmann Institute of Science, Rehovot, Israel

Received 14 June 2004/Returned for modification 13 September 2004/Accepted 30 September 2004

A major function of TFIID is core promoter recognition. TFIID consists of TATA-binding protein (TBP) and 14 TBP-associated factors (TAFs). Most of them contain a histone fold domain (HFD) that lacks the DNA-contacting residues of histones. Whether and how TAF HFDs contribute to core promoter DNA binding are yet unresolved. Here we examined the DNA binding activity of TAF9, TAF6, TAF4b, and TAF12, which are related to histones H3, H4, H2A, and H2B, respectively. Each of these TAFs has intrinsic DNA binding activity adjacent to or within the HFD. The DNA binding domains were mapped to evolutionarily conserved and essential regions. Remarkably, HFD-mediated interaction enhanced the DNA binding activity of each of the TAF6-TAF9 and TAF4b-TAF12 pairs and of a histone-like octamer complex composed of the four TAFs. Furthermore, HFD-mediated interaction stimulated sequence-specific binding by TAF6 and TAF9. These results suggest that TAF HFDs merge with other conserved domains for efficient and specific core promoter binding.

Transcription of protein-encoding genes in eukaryotes involves the assembly of RNA polymerase II and general transcription factors (GTFs) on the core promoter to form a preinitiation complex (PIC). TFIID is the major DNA-binding GTF. It is composed of the TATA-binding protein (TBP) and 14 TBP-associated factors (TAFs). TAFs regulate transcription at multiple levels. Certain TAFs interact with activators to facilitate PIC formation (2, 18) and transcription reinitiation (1). TAFs also have a role in recognition and binding to core promoter elements. DNase I footprinting revealed direct contact of TAFs with sequences upstream and downstream of the TATA box (11, 19, 23, 26, 29, 35). TAF1-TAF2 ($TAF_{II}250$-$TAF_{II}150$) binds the Initiator element (7, 33, 34), multiple TAFs were cross-linked to the adenovirus major late (AdML) promoter (24), and *Drosophila melanogaster* TAF6 (dTAF6) and dTAF9 ($dTAF_{II}60$-$dTAF_{II}42$) were cross-linked to the downstream promoter element (DPE) (5). Some TAFs are TFIID specific, but others are shared by other transcription regulatory complexes (3, 4, 15, 22, 25, 28).

One common feature found in 9 out of the 14 TAFs is the histone fold motif (for a review see reference 13). This motif has been established as an essential protein-protein interaction domain that facilitates assembly of TFIID in a manner analogous to that for histones (17, 30). TAF6 and TAF9 are structurally related to histones H4 and H3, respectively (38). TAF12 is similar to H2B, TAF4 contains an H2A-like domain, and both interact with each other via the histone fold domain (HFD) (14, 16, 30). In vitro *Saccharomyces cerevisiae* TAF6 (yTAF6)-yTAF9 can assemble with yTAF12-yTAF4 to form a histone octamer-like structure (30).

The nucleosome-like interaction of TFIID with DNA (24) and the presence of histone fold TAFs within this complex have led to the proposal that a nucleosome-like octamer within TFIID may be involved in direct DNA binding (17). However, the issue has remained elusive. First, there is no experimental evidence for DNA binding by the TAF histone fold motif. Second, some of the surface residues in histones H3-H4 and H2A-H2B that contact DNA in the nucleosome are not conserved in the TAF6-TAF9 and TAF4-TAF12 complexes, as revealed from their crystal structures (36, 38). In addition, the surface-exposed area of the TAF4-TAF12 complex is mostly negatively charged and therefore considered to lack DNA binding activity (36). Thus, to date it is unknown whether the HFDs of TAFs are involved in core promoter binding by TFIID.

In the present study we tested whether the H3-H4-like TAF9-TAF6 and the H2A-H2B-like TAF4b-TAF12 display DNA binding activity and what is the role of their HFDs in this activity. Our results show that the HFDs of TAFs contribute in various ways to core promoter binding by TFIID.

MATERIALS AND METHODS

Construction of recombinant plasmids. To generate expression plasmids for glutathione *S*-transferase (GST)-tagged human TAF6 (hTAF6), hTAF9, hTAF4b, hTAF4, dTAF4, and their mutant derivatives, the DNA encoding these regions was amplified by PCR with oligonucleotide primers with restriction sites from the appropriate plasmids. The PCR fragments were cloned into the pGEX-2TKN expression vector. The hTAF12 full-length cDNA was obtained from a yeast two-hybrid screen for genes that interact with the C-terminal domain of hTAF4b. To construct six-His-tagged-TAF12, the cDNA (BglII fragment) was cloned in the BamHI site of pET-28c. yTAF4 was amplified from a yeast genomic library (a gift from Jeffrey Gerst, Weizmann Institute of Science) and cloned into the pGEX-2TKN vector to generate GST fusion proteins. Mutant yTAF4 coding sequences were constructed by PCR and then cloned into pGEX-2TKN and into the high-copy-number yeast expression plasmid pAD54, which encodes the LEU2 marker. All the recombinant plasmids were verified by sequencing.

* Corresponding author. Mailing address: Department of Biological Chemistry, The Weizmann Institute of Science, Rehovot 76100, Israel. Phone: 972-8-9342117. Fax: 972-8-9344118. E-mail: rivka.dikstein@weizmann.ac.il.

† H.S. and M.R. contributed equally to this study.

‡ Present address: Department of Pathology, University of Pittsburgh, Pittsburgh, Pa.

Protein expression and purification. hTAF6, hTAF9, hTAF4b, hTAF4, dTAF4, yTAF4, and hTAF12 and all their mutant derivatives were expressed in the BL-21(DE3) strain and, with the exception of TAF6 500–677, were found in the insoluble fraction (inclusion bodies). Cells were grown at 37°C up to an optical density at 600 nm of 0.6 to 0.8 and then induced by 0.2 mM IPTG (isopropyl-β-D-thiogalactopyranoside) for an additional 3 h. The cell pellet was resuspended in phosphate-buffered saline (PBS) and subjected to a 30-s sonication three times. The inclusion bodies were washed once with PBS, dissolved in dialysis buffer (10 mM Tris-Cl [pH 8.0], 100 mM KCl, 0.1 mM EDTA, 10 mM β-Met) containing 8 M urea, and dialyzed against 100 volumes of dialysis buffer with 1 M urea and twice against 100 volumes of dialysis buffer without urea, with the final dialysis in a buffer containing 20% glycerol. For the purifications of refolded and soluble proteins, all supernatants were incubated with glutathione-agarose beads in GST binding buffer at 4°C for 45 min. The beads were washed four times with binding buffer, and bound proteins were eluted by incubating them in 10 mM glutathione–50 mM Tris-Cl, pH 8.0, on a rotator for 10 min. The eluate was collected and dialyzed once against 100 volumes of dialysis buffer for 2 h and once against dialysis buffer containing 20% glycerol for 4 h. For the preparation of the TAF6-TAF9 complex similar amounts of denatured TAF6 and TAF9 were mixed, refolded, and purified through GST beads. The TAF4b-TAF12 complex was similarly refolded and purified, first on nickel-agarose (QIAGEN) and then on glutathione-Sepharose.

DNA binding assays. The proteins were incubated with either empty or DNA-bound beads (1.0 μg of biotinylated DNA fragment bound to magnetic beads or 0.24 to 1.0 μg of DNA bound to cellulose beads [double-stranded calf thymus DNA; Sigma; catalog no. D-8515]) for 45 min, at room temperature, in binding buffer containing 10 mM Tris (pH 8.0), 50 mM KCl, 2.5 mM dithiothreitol (DTT), 0.1 mg of bovine serum albumin (BSA)/ml, 15% glycerol, and 0.2% NP-40. The beads were then washed three times with binding buffer, and the proteins were eluted with 30 μl of binding buffer containing 1 M NaCl. The bound proteins were analyzed by sodium dodecyl sulfate-polyacrylamide gel electrophoresis (SDS-PAGE), followed by silver staining. The DNA used for the electrophoresis mobility shift assays (EMSA) with TAF6 and TAF9 and the putative TAF octamer was derived from the IRF-1 promoter containing DPE with the following sequence: 5′-AGAGCTCGCCACTCCTTAGTCGAGGCAAGACGTGCGCCCGAGCCCCGCCGAACCGAGGCC-3′. The DPE site is underlined. The DNA sequence of mutant DPE was 5′-AGAGCTCGCCACTCCTTAGTCGAGGCATATGCATCGCCCGAGCCCCGCCGAACCGAGGCC-3′. DNA was labeled by [γ-^{32}P]ATP (Amersham Biosciences) and polynucleotide kinase and precipitated by ethanol. For the binding reaction, a DNA probe (2 ng) was incubated with the proteins in a 20-μl reaction mixture in DNA binding buffer containing 10 mM Tris, pH 8.0, 75 mM KCl, 2.5 mM DTT, 0.1 mg of BSA/ml, 15% glycerol, and 0.05% NP-40 for 20 min at room temperature and then was loaded onto a 5% native polyacrylamide gel containing 0.5× Tris-borate-EDTA buffer. The gel was dried and visualized with a PhosphorImager (Fugi; BAS 2500). For supershift experiments, the antibodies were preincubated with the protein for 5 min prior to the addition of the DNA probe. Anti-TAF9 and anti-TAF1 antibodies were purchased from Santa Cruz Biotechnology Inc. The anti-TAF12 monoclonal antibody is a gift from Irwin Davidson (Centre National de la Recherche Scientifique [CNRS], Strasbourg, France), and anti-TAF6 was generously provided by Laszlo Tora (CNRS). For the EMSA experiments with TAF4b, either the J-chain or the IRF-1 core promoters were used.

UV cross-linking experiments. The TAF4b-TFIID complex was immunoprecipitated from Daudi nuclear extract in D/NP-40 buffer (20 mM HEPES [pH 7.9], 100 mM KCl, 2 mM $MgCl_2$, 0.2 mM EDTA, 20% glycerol, 0.1% NP-40) with TAF4b-specific antibodies (27) or control antibodies. The labeled major late promoter was generated by 20 cycles of PCR with [α-^{32}P]ATP and the primers 5′-GTGACTTTGTGTTCCTGAAGGGGGGC-3′ and 5′-CCATGATTACGCCAAGCTTGCATC-3′. Labeled DNA was recovered by ethanol precipitation and then incubated with the immunoprecipitated proteins in binding buffer [20 mM HEPES (pH 7.9), 50 mM NaCl, 10% glycerol, 2% polyethylene glycol 8000, 5 mM $(NH_4)_2SO_4$, 5 mM $MgCl_2$, 3 mM 2-mercaptoethanol, 100 μg of BSA/ml] at room temperature for 30 min. The binding reaction mixture was then irradiated by a 366-nm UV lamp from a distance of 5 cm for 10 min. DNase I buffer and 1 U of RQ1 DNase I were added (Promega), and the mixture was incubated at 37°C for 15 min. The unbound DNA fragments were washed off the beads, and proteins were eluted with sample buffer and 5 min of boiling.

Immunoprecipitation. Proteins were incubated with antibodies at 4°C for 30 min and then transferred to a clean tube containing a mixture of protein A and protein G beads equilibrated with DNA binding buffer. After a 30-min rotation at 4°C the beads were washed with DNA binding buffer. The beads were resuspended in 1× sample buffer, boiled 3 min, and subjected to SDS-PAGE and silver staining.

Yeast complementation and growth assays. The TAF4 null strain used in this study was YSLS46 (*MAT***a** *leu2Δ0 ura3Δ0 his3Δ1 met15Δ0 KANΔtaf4* [pRS416ADH-TAF4]). It was grown in yeast extract-peptone-dextrose medium plus kanamycin and was transformed by plasmids encoding TAF4 mutant derivatives by the lithium acetate procedure. Transformed yeast cells were selected on synthetic dextrose medium (SD) lacking leucine (SD−leucine). The yTAF4URA3 plasmid was then shuffled out by growing the cells on SD−leucine containing 1 mg of 5-fluoroorotic acid (5-FOA; Sigma) for 5 days at 25°C. Shuffled cells were transferred again to plates containing SD−leucine plus 5-FOA and grown at 25 and 37°C.

Preparation and analysis of RNA. Total RNA from yeast cells at the logarithmic phase of growth was prepared as described previously (32). Equivalent amounts of RNA (0.7 and 1.4 μg) were dot blotted onto a nitrocellulose membrane, fixed, and hybridized with a labeled oligo$(dT)_{20}$ probe.

RESULTS

TAF9 binds DNA directly through a highly conserved functional domain. TAF9 and TAF6 form an H3-H4-like heterotetramer that lacks the conserved DNA-contacting residues (38). TAF9 contains several domains (Fig. 1A): a highly conserved N-terminal HFD (amino acids 13 to 74), important for interaction with the H4-like TAF6, another conserved region (CR), which flanks the HFD (amino acids 75 to 135), with unknown function, and a long less-conserved C-terminal tail (amino acids 136 to 264), which is absent from yTAF9. Recent complementation analysis of chicken TAF9 (cTAF9) null cells revealed that the HFD and the CR domains are sufficient for cellular growth and that both of these domains, but not the C-terminal tail, are essential (8).

To examine TAF9 and TAF6 for DNA binding activity and determine the role, if any, of their HFDs, we used the immobilized-DNA-binding assay. Different segments of TAF9 were expressed in *Escherichia coli* and analyzed for binding to either DNA-cellulose or empty cellulose beads, which served as a control (Fig. 1B). The results showed that full-length TAF9 binds specifically to the DNA beads, suggesting that it has intrinsic DNA binding activity. Importantly, TAF9 fragments lacking either the HFD (TAF9 75–264) or the C-terminal tail (TAF9 1–137) do not lose DNA binding activity. By contrast, any deletion of the CR domain abolishes the DNA binding activity (TAF9 1–120 and TAF9 137–264). The minimal DNA binding activity was mapped to the evolutionarily conserved CR domain, consisting of amino acids 70 to 147 (Fig. 1B, lanes 19 to 21). Given that cTAF9 lacking the CR domain failed to complement the cell growth defect of cTAF9 null cells (8), TAF9 binding to DNA appears to be an essential function in vivo.

TAF6 has intrinsic DNA binding activity localized C terminal to the HFD. A similar analysis of hTAF6, the H4-like partner of the H3-like TAF9 (Fig. 1C), showed that TAF6 also binds to DNA-cellulose. Like TAF9, a protein fragment lacking the HFD (TAF6 78–542) still binds DNA, so DNA binding activity resides C terminal to the HFD. Like TAF9, the HFD of TAF6 (Fig. 1C, lanes 1 to 3) failed to bind to DNA-cellulose, indicating that the TAF6-TAF9 histone fold complex lacks intrinsic DNA binding activity. The inability of TAF6 and TAF9 HFDs to bind DNA is in agreement with the absence of conservation in the DNA contacting residues between histones H3-H4 and the HFDs of TAF6 and TAF9 (38). The DNA

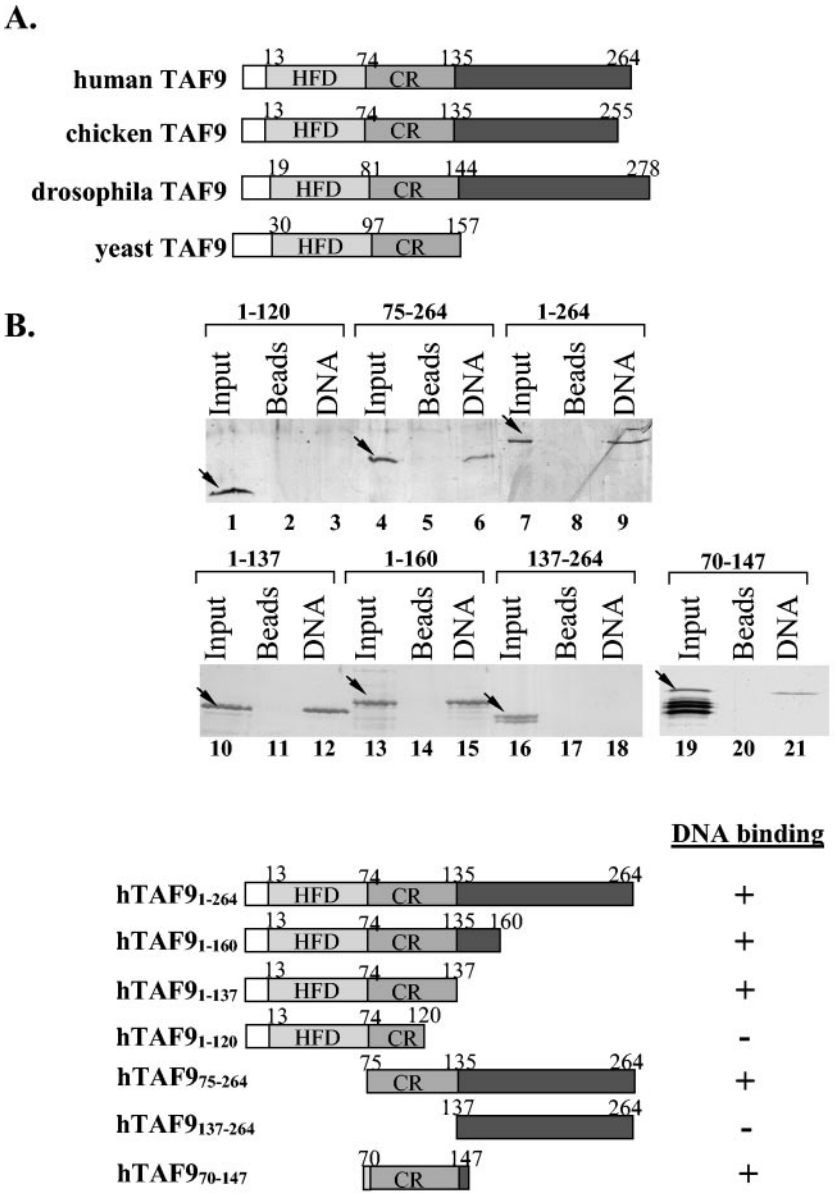

FIG. 1. TAF6 and TAF9 have intrinsic DNA binding activity localized C-terminal to the histone fold motif. (A) Schematic representation of the homology between TAF9s of different species. The positions of the HFD, the neighboring CR, and the less conserved C terminus are shown. (B) Full-length human TAF9 and different mutant versions were constructed as GST fusion proteins, expressed in *E. coli*, and analyzed for binding to DNA-cellulose beads (DNA lanes). Binding to empty cellulose beads (bead lanes) served as a control. The input represents 10% of the protein used for binding. The bound proteins were eluted with binding buffer containing 1 M NaCl, and 20% of the eluted proteins was analyzed by SDS-PAGE and silver staining. The protein fragments used for the binding assays are indicated at the top. Arrows, positions of the protein used for the DNA binding assay. A schematic representation of TAF9 derivatives used to define the DNA binding domain is at the bottom. +, positive DNA binding; −, undetectable DNA binding. (C) Different regions of human TAF6 (as indicated) were analyzed for DNA binding as was done for TAF9 in panel B. A schematic representation of binding results is shown at the bottom.

binding region of TAF6 was mapped to amino acids 300 to 400 within an evolutionarily conserved region (Fig. 1C).

Interaction of TAF6-TAF9 through the HFD greatly enhances DNA binding activity. To investigate further the DNA binding activity of TAF6 and TAF9, we performed EMSA. EMSA is more stringent than the DNA-cellulose binding assay, as it requires formation of a protein-DNA complex that can withstand an electric field. We used purified TAF6 and TAF9 derivatives either alone or as a complex (Fig. 2B). These proteins were incubated with a 60-bp DNA fragment composed of the human IRF-1 downstream promoter region, which bears a functional DPE (5). As shown in Fig. 2A a protein-DNA complex was detected by this assay with full-length (lane 3) or histone fold-deleted TAF9 (lane 8), confirming that TAF9 DNA binding resides outside the HFD. A complex consisting of only the HFDs of TAF6 and TAF9 (TAF6 1–160 and TAF9 1–120) failed to bind DNA (lane 4). TAF6 1–400 and 78–542 (lanes 2 and 7) failed to produce protein-

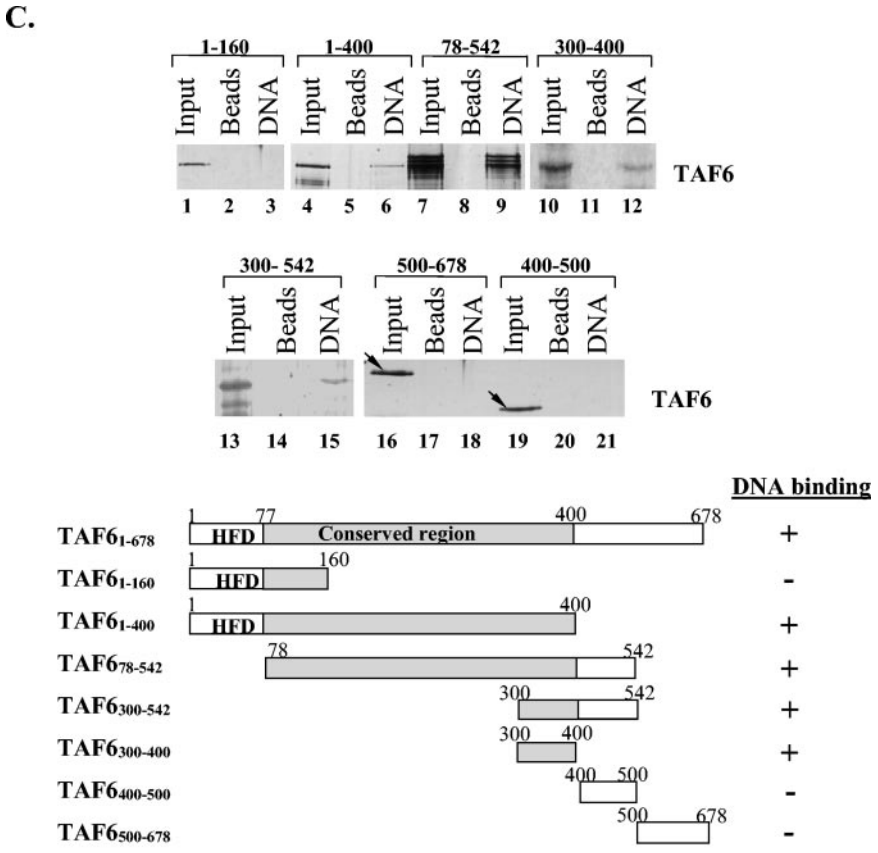

FIG. 1—*Continued*.

DNA complexes, even though these proteins did bind DNA-cellulose, suggesting that the TAF6-DNA complex is not stable enough for EMSA. However, a complex composed of TAF6 1–400 and full-length TAF9 displayed much greater DNA binding activity than either of them alone (lane 5), whereas no effect on DNA binding activity was seen with the two proteins without their HFDs (lanes 7 to 9). Quantification of the bound DNA indicated that interaction of TAF6 with TAF9 increased the amount of DNA-bound TAF9 by 11-fold. We then used TAF9-, TAF6-, or TAF12-specific antibodies to verify the presence of TAF9 and TAF6 in the band corresponding to the TAF6-TAF9 complex. We found that TAF9 antibodies specifically inhibited the formation of the DNA-protein complex and that TAF6 antibodies reduced the mobility of the complex, while the TAF12 antibody has no effect on this complex (Fig. 2C). The effect of TAF9 antibodies is specific, as they did not affect a protein-DNA complex lacking TAF9 (see Fig. 8B). To confirm that TAF6 associates with TAF9, we performed coimmunoprecipitation of the TAF6-TAF9 protein mixture using either TAF9- or TAF1-specific antibodies and found that both proteins were specifically precipitated by TAF9 antibodies but not TAF1 antibodies (Fig. 2D). As TAF6 and TAF9 interact with each other through their HFDs, we conclude that, although these HFDs do not directly bind DNA, they dramatically enhance DNA binding activity.

Interaction of TAF6-TAF9 via the HFD contributes to DPE-specific binding. To examine the sequence specificity of these TAFs for the DPE, we performed competition experiments with increasing amounts of nonlabeled wild-type or DPE-mutated DNAs. We used TAF9 alone or in a complex with TAF6. With TAF9 alone wild-type and mutated DPE competed equally with the labeled DNA (Fig. 3A). By contrast, the TAF6-TAF9 complex clearly discriminated between them, as the wild type competed more effectively than the mutated DPE (Fig. 3B). DNAs that were mutated in the sequence that flanks the DPE motif competed as effectively as the wild-type DNA for TAF6-TAF9 binding (Fig. 3C), further confirming the preference for the DPE. Therefore, DPE-specific binding is dependent on TAF6 and TAF9 as a complex and the HFD-mediated interaction between TAF6 and TAF9 contributes not only to the extent of the DNA binding activity, as shown in Fig. 2A, but also to sequence specificity.

DNA binding by the H2A-like hTAF4b ($TAF_{II}105$). TAF4b ($TAF_{II}105$) is a substoichiometric TFIID-specific subunit whose expression is regulated in a tissue-specific manner (10, 12, 31). TAF4b is a member of the TAF4 family ($hTAF_{II}135$, $dTAF_{II}110$, and yTAF48p) that shares a highly conserved C-terminal domain, important for interaction with other TAFs (31) and containing an H2A-like HFD (14, 16). The N terminus of TAF4b is less conserved and is required for interaction with activators (31, 37, 39). To examine whether hTAF4b has intrinsic DNA binding activity, the immobilized DNA binding assay was applied. As shown in Fig. 4A (top), hTAF4b was specifically retained on the DNA-containing beads, suggesting

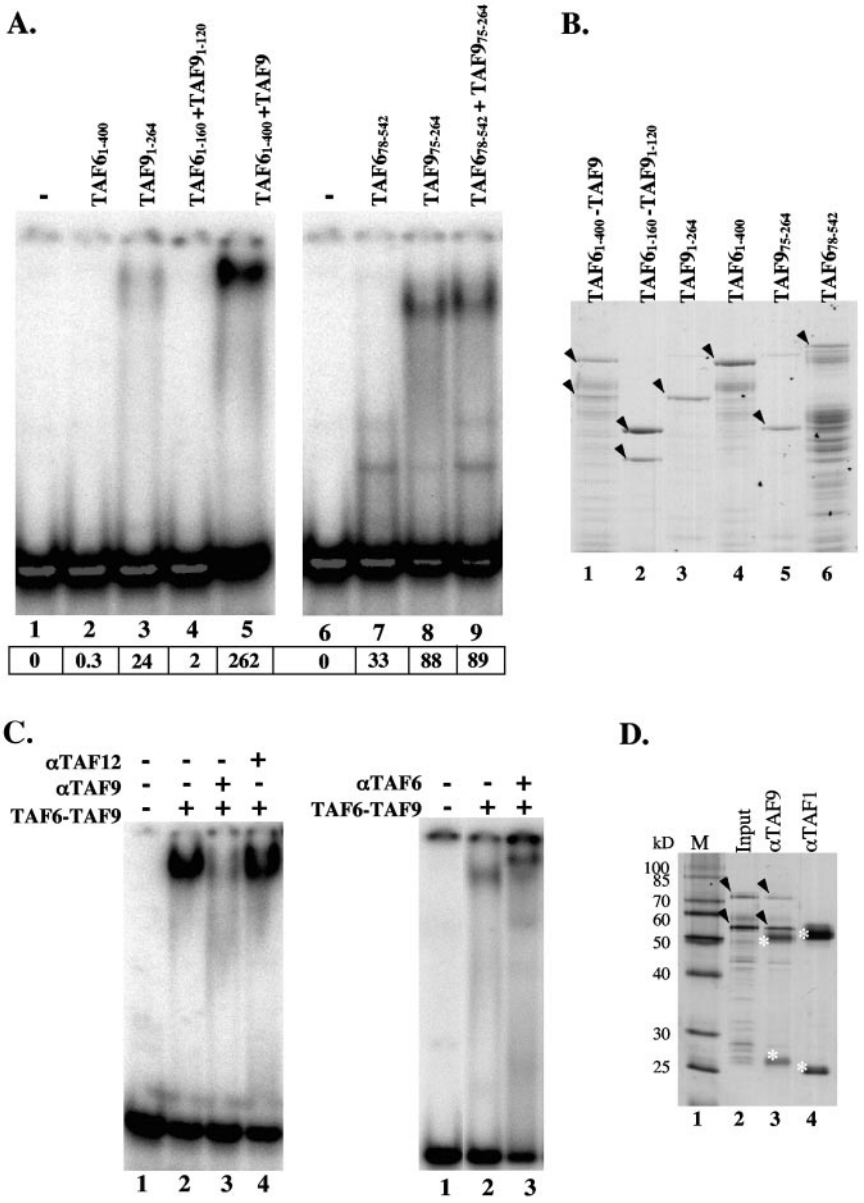

FIG. 2. Interaction of TAF6 and TAF9 through the HFD enhances DNA binding. (A) Analysis of the DNA binding of purified TAF6 and TAF9 protein derivatives either alone or as a complex by EMSA. The bound DNA was quantified, and results are presented as densitometric units (bottom). The probe was the DPE-containing IRF-1 downstream promoter DNA. (B) Analysis of the proteins used for the EMSA by SDS-PAGE and Coomassie staining. The amount loaded on this gel is threefold higher than that used for EMSA. (C) Analysis of the TAF6-TAF9 complex by antibodies. The indicated antibodies were preincubated with the TAF6-TAF9 complex and then used for EMSA. (D) Coimmunoprecipitation experiment of the TAF6-TAF9 complex, with either TAF9-specific polyclonal antibodies or a TAF1 monoclonal antibody as a negative control. The input (5%) and the immunoprecipitated proteins were analyzed by SDS-PAGE and silver staining. Arrowheads, positions of TAF6 and TAF9; asterisks, positions of the heavy and light chains of the antibodies.

that it has DNA binding activity. To determine which of the hTAF4b functional domains bears the DNA binding activity, the diverged N-terminal domain and the conserved C terminus were expressed in *E. coli* and analyzed for DNA binding (Fig. 4A, middle and bottom). This experiment indicates that DNA binding activity resides within the C-terminal domain of hTAF4b.

Since the C-terminal DNA binding domain of TAF4b is expressed in *E. coli* as an insoluble protein that is refolded by a denaturation-renaturation procedure, we confirmed that it refolded properly by testing its ability to interact with all the known interacting proteins, hTAF1 (TAFII250), hTAF12 (TAFII20), and hTFIIA, by a GST pull-down assay (Fig. 4B).

To determine whether TAF4b binds DNA in its native TFIID context, the TFIID complex was affinity purified from Daudi B-cell nuclear extract with TAF4b-specific antibodies (10). The purified TAF4b-TFIID complex was reacted with a labeled DNA fragment containing the AdML core promoter

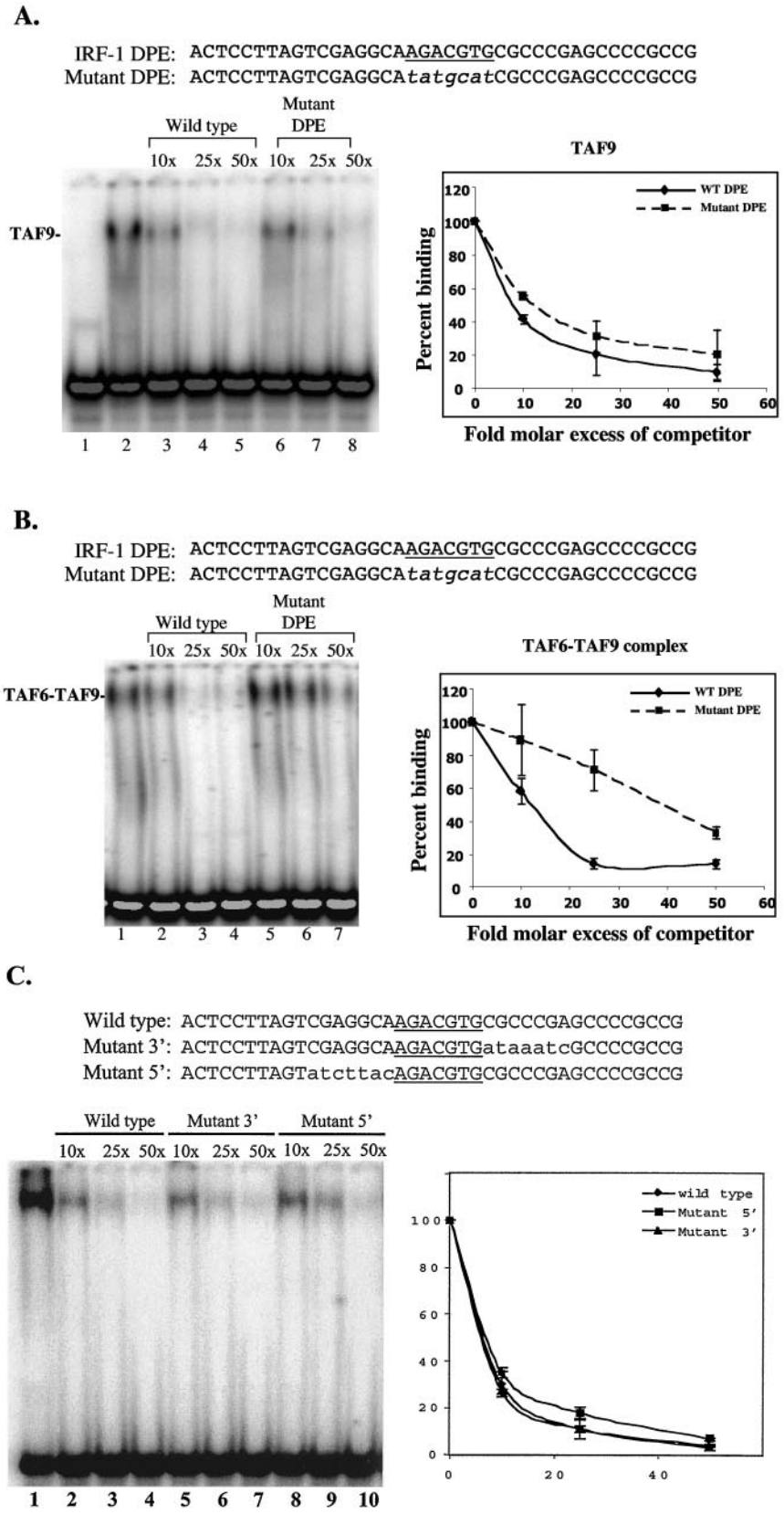

FIG. 3. Analysis of sequence specificity for the core promoter element DPE. (A) TAF9 was subjected to DNA binding competition assays using the labeled IRF-1 probe and the indicated excess amounts of nonlabeled DNAs composed of either wild-type or mutated DPE (sequences are shown at the top). Graphic presentations of the quantified competition results are shown on the right. (B and C) TAF6-TAF9 complex was subjected to DNA binding competition assays using labeled IRF-1 probe and the indicated excess amounts of nonlabeled DNAs composed of either wild-type or mutant oligonucleotides. The sequences used are shown on the top. The DPE is underlined, and mutated bases are in lowercase. The graphs represent the means ± standard deviations of two or three independent experiments.

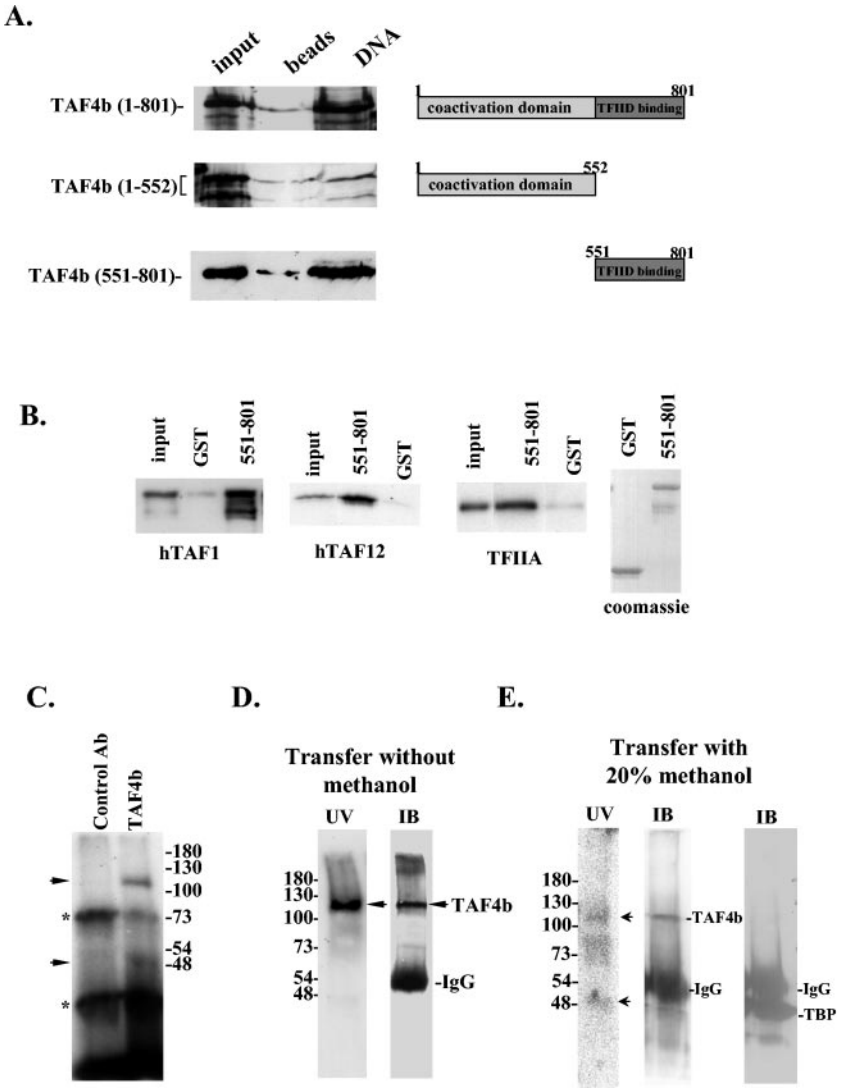

FIG. 4. hTAF4b has intrinsic DNA binding activity. (A) Full-length hTAF4b and N- and C-terminal fragments of hTAF4b were analyzed for binding to a DNA fragment containing the A20 promoter, which was biotinylated and immobilized on streptavidin-coated magnetic beads. A control binding reaction was conducted with empty beads. The bound protein was eluted by 1 M NaCl and analyzed by immunoblotting with either N-terminus-specific anti-hTAF4b antibodies for the full-length protein and the N terminus (TAF4b 1–801 and 1–552, respectively) or anti-GST antibodies to detect the C-terminal (TAF4b 551–801) fragment. The input represents 5% of the amount used for the binding reaction. (B) GST pull-down assay using GST or GST fused to hTAF4b 551–801 immobilized on glutathione beads. The amounts of the immobilized proteins used for the binding reactions are shown by the Coomassie blue-stained SDS-PAGE gel (right). In the left panel the binding reaction was performed with cell extract from SF9 cells expressing hemagglutinin (HA)-tagged hTAF1 ($hTAF_{II}250$). The eluted proteins were analyzed for TAF1 binding by immunoblotting with an anti-HA antibody. In the next panels the binding was carried out with the in vitro-translated and ^{35}S-labeled TAF12 and TFIIA large subunits. The bound proteins were subjected to SDS-PAGE, followed by autoradiography. Input represents 10% of the amount of protein used for binding. (C) TAF4b in the context of TFIID is cross-linked to the MLP promoter. Daudi B-cell nuclear extract was used for immunoprecipitation of TAF4b-TFIID with TAF4b-specific antibodies (Ab) or control immunoprecipitation with nonrelevant antibodies (anti-invertase). The immunoprecipitated complexes were subjected to a binding reaction with the labeled AdML promoter, followed by UV cross-linking, nuclease digestion, and SDS-PAGE. Arrowheads, specific cross-linked polypeptides; asterisks, nonspecific bands. (D) A UV cross-linking experiment similar to that for panel C was run on two lanes of the same gel. Immunoprecipitated complexes were blotted onto nitrocellulose paper. One lane was exposed to X-ray film (UV), and the second was subjected to immunoblot analysis using TAF4b-specific antibodies (IB). Arrowheads, TAF4b and the cross-linked polypeptide. (E) Cross-linking experiment similar to that for panel C. Immunoprecipitated complexes were transferred onto a nitrocellulose membrane in the presence of 20% methanol. After the autoradiography (UV lane) the membrane was subjected to immunoblotting with TAF4b- and TBP-specific antibodies (IB lanes).

(from −48 to +1) and then subjected to UV cross-linking and nuclease digestion. Two polypeptides specifically cross-linked to the DNA in TAF4b-TFIID but not in the control immunoprecipitation. The major polypeptide was approximately 110 kDa, and the second was 48 kDa (Fig. 4C). The absence of cross-linked polypeptides corresponding to hTAF1 and hTAF2 ($TAF_{II}250$ and $TAF_{II}150$, respectively) is possibly due to the fact that the promoter fragment that we used lacks part of the

Initiator sequence. The only known polypeptide in TAF4b-TFIID that has a size similar to that of the 110-kDa cross-linked band is TAF4b. The 48-kDa polypeptide has a mobility similar to that of TBP by SDS-PAGE. The two nonspecific bands are most likely nuclease-resistant DNA molecules, as they did not bind nitrocellulose (Fig. 4D) and appeared in UV cross-linking in the absence of proteins (data not shown). To determine whether the 110-kDa DNA binding polypeptide is TAF4b, products from a similar UV cross-linking experiment were loaded onto two lanes of the same gel and transferred to nitrocellulose paper under conditions that favor transfer of large proteins. One was subjected to autoradiography, and the second was subjected to immunoblot analysis with TAF4b-specific antibodies, so the mobility of the cross-linked 110-kDa polypeptide could be compared to that of immunoreactive TAF4b. As shown in Fig. 4D (right), the DNA-cross-linked polypeptide has exactly the same mobility as TAF4b. The second 48-kDa band was seen after longer exposure. To confirm that the 48-kDa band represents TBP, we repeated the experiment and used transfer conditions (20% methanol) that favor retention of small proteins on the membrane (Fig. 4E). The 110- and 48-kDa bands comigrate with TAF4b and TBP, respectively. These results suggest that TAF4b binds DNA directly in the context of TFIID-like TBP.

TAF4b has an atypical histone fold motif that is required for DNA binding. The C-terminal domain of the TAF4 family contains several elements: an H2A-like HFD essential for interaction with the H2B-like TAF12 (14–16), a predicted coiled-coil domain, and surfaces for interaction with other proteins. Since the analyses of the yTAF4-yTAF12 and hTAF4-hTAF12 pairs have yielded conflicting results with respect to the importance of the most C-terminal region of TAF4 for TAF12 interaction (14, 32, 36), we mapped the C-terminal boundary of hTAF4b required for interaction with TAF12 and found that the last 31 amino acids significantly contribute to the efficiency of the association with TAF12 (data not shown). Thus, our results are consistent with the requirement for the extreme C-terminal domain of yTAF4, termed CCTD, for interaction with yTAF12 (32) and support the idea that the CCTD contains the genuine third alpha helix of the histone fold (32). The putative third helix is separated from the second helix by an unusually long spacer domain, suggesting that hTAF4b has an atypical histone fold arrangement, as shown schematically in Fig. 5B.

To map the regions within hTAF4b directing the DNA binding activity, we examined N- and C-terminal truncations for binding to either empty or DNA-containing cellulose beads. The mapping of the DNA binding activity is shown in Fig. 5A and is summarized in Fig. 5B. Analysis of mutant proteins with C-terminal truncations suggests that the DNA binding activity requires amino acids 735 to 769 of the unique spacer domain but neither the coiled-coil motif of this domain nor the third helix of the histone fold. Dissection of the N-terminal domain revealed that DNA binding was unaffected by deleting the regions before the first helix (hTAF4b 596–801), the first helix (α1;hTAF4b 609–801), and the first loop (L1;hTAF4b 618–801) but that it was abolished by a further deletion of the first 13 amino acids (hTAF4b 631–801) from the second helix (α2) (Fig. 5A and B). On disruption of the other half of the α2 helix by two proline substitutions (L631P and L634P) DNA binding was retained even though interaction with TAF12 was severely compromised (32). Deletion of the third helix (α3) also interfered with the interaction with TAF12 (data not shown) but not with DNA (Fig. 5A and B). Therefore it can be concluded that the binding of hTAF4b to TAF12 and its binding to DNA are independent of each other. In summary, DNA binding by hTAF4b involves the HFD and an additional region, the unique spacer domain. However, the mode of DNA binding by hTAF4b is different from that of histone H2A because, in contrast to those of hTAF4b, many of the DNA contacts in histone H2A are through the first helix and the first loop but not the second helix (21). These results explain why the DNA contacting residues in α1 and L1 of H2A were not preserved in TAF4 family members.

To gain further support for TAF4b DNA binding activity, we analyzed some TAF4b mutant derivatives by EMSA. As in the DNA-cellulose binding assays, TAF4b 551-769 bound DNA (Fig. 5C) whereas equal amounts of mutant derivatives of TAF4b lacking parts of the spacer domain, TAF4b 551-734 and Δ735-769, failed to bind DNA (Fig. 5C). The TAF4b protein-DNA complex seems to dissociate during electrophoresis, as evident from the extended edges of the complex in lane 2.

DNA binding activity is conserved among TAF4 orthologs. The DNA binding region of hTAF4b is highly homologous to the C termini of hTAF4 and TAF4 from different organisms. We therefore examined whether TAF4 from different species also display DNA binding activity. The C termini of hTAF4 ($hTAF_{II}135$), dTAF4 ($dTAF_{II}110$), and yTAF4 (yTAF48p) were cloned, expressed in *E. coli*, and then analyzed for binding to either cellulose or DNA-cellulose beads. As shown in Fig. 6A hTAF4b, hTAF4, dTAF4, and yTAF4 were all specifically retained on DNA-cellulose, indicating that their DNA binding activity is conserved throughout the TAF4 family and thus may be important.

Analysis of hTAF4b DNA binding indicated that part of the unique spacer domain is necessary for its DNA binding activity. To examine whether this region in the yTAF4 protein is also required for the DNA binding activity, we used the previously reported alignment between TAF4 members (32) to construct yTAF4 deletion mutant proteins that are equivalent to mutant proteins hTAF4b 551–769 and 551–801Δ735–769, shown in Fig. 5. These yeast mutant proteins were analyzed for DNA binding (Fig. 6B). Like that by hTAF4b, DNA binding by yTAF4 was unaffected by removal of the extreme C terminus (CCTD) but was significantly impaired by partial deletion of the spacer region. These findings further confirm the conserved nature of TAF4 DNA binding activity.

DNA binding activity is an essential function of yTAF4. yTAF4 is essential for normal yeast growth (27). A recent study analyzed the abilities of various yTAF4 mutants to compensate for the loss of the yTAF4 gene (32) and found that the regions that participate in yTAF4's interaction with yTAF12 are critical for the normal function of yTAF4. The entire spacer domain between the second and the third helices of the histone fold, which is not required for interaction with TAF12, was also vital for yTAF4 function. As we found a small region within this spacer domain to be indispensable for both hTAF4b and yTAF4 DNA binding activity, it is possible that DNA binding by yTAF4 is an important function. To address this possibility, we analyzed, by plasmid shuffling experiments, the ability of a

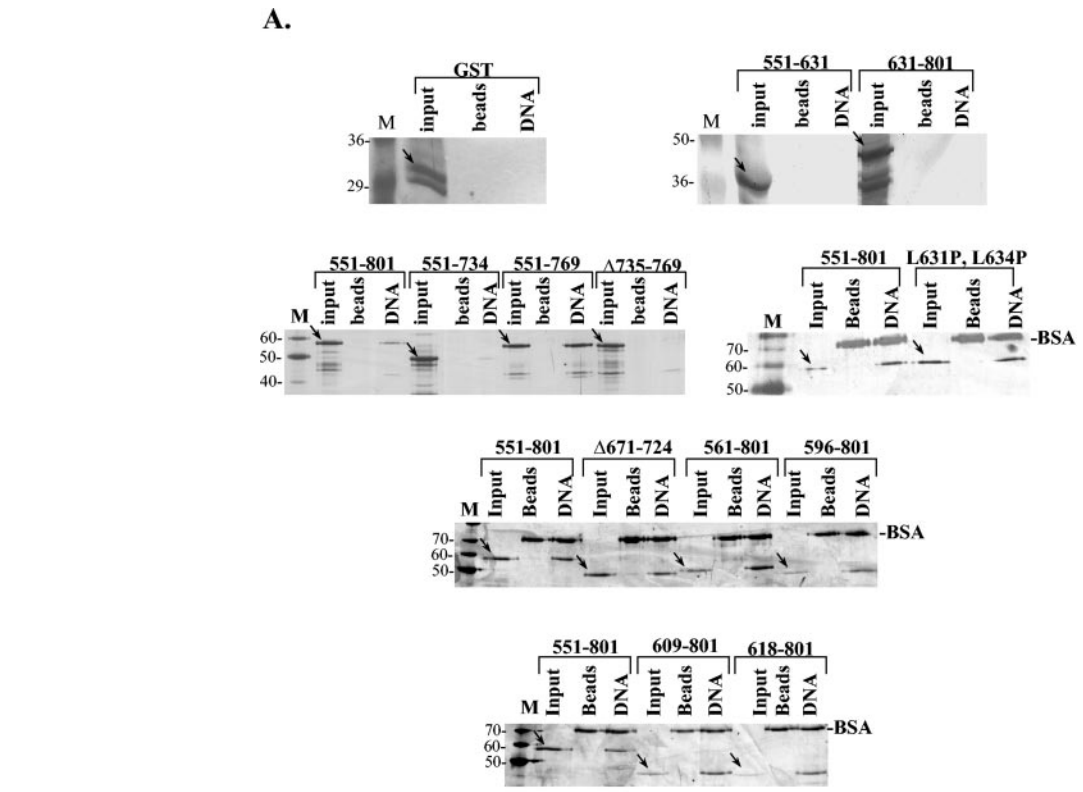

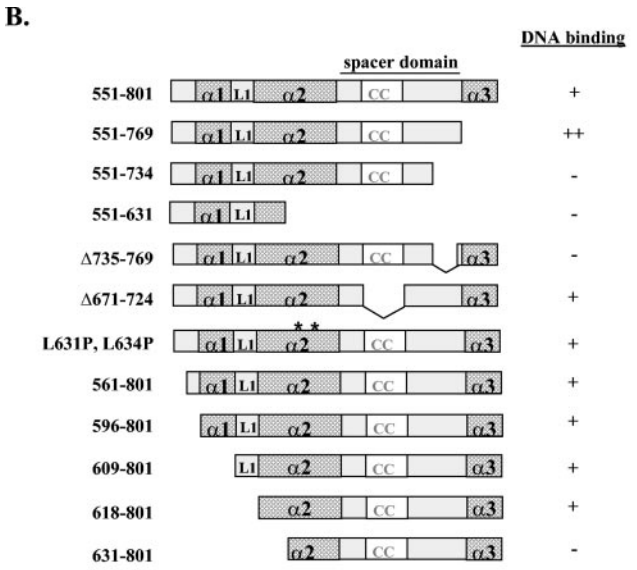

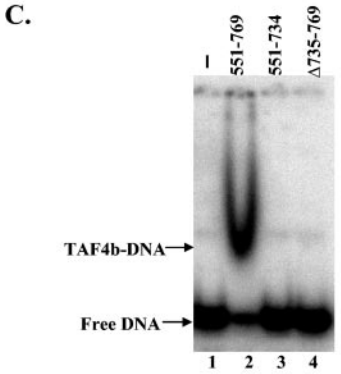

FIG. 5. Mapping of hTAF4b DNA binding region. (A) Different hTAF4b mutant derivatives were constructed as GST fusion proteins and analyzed for binding to DNA-cellulose beads (DNA lanes). A control binding reaction was done with empty cellulose beads (beads lanes). The input represents 5% of the protein used for binding. The bound proteins were eluted with binding buffer containing 1 M NaCl, and 20% was analyzed by SDS-PAGE and silver staining. The proteins used for the binding assays are indicated at the top. DNA binding by the GST protein is used as a specificity control (left). M, protein size marker; arrows, positions of the protein used for the DNA binding assay. The position of BSA, present in the binding buffer, is indicated. (B) Schematic representation of hTAF4b mutant derivatives used to define the DNA binding domain by applying the DNA-cellulose binding assay. +, DNA binding; −, undetectable DNA binding. (C) DNA binding analysis by EMSA of purified hTAF4b mutant derivatives (50 ng each) using the J chain core promoter, which was previously shown to be regulated by TAF4b, as a probe (37). TAF4b mutant derivatives are TAF4b 551–769, 551–734, and 551–801Δ735–769, as indicated at the top of each lane.

DNA binding mutant yTAF4 protein to rescue the growth of a yeast strain deficient in the TAF4 gene. A TAF4 null strain was rescued by both yTAF4 151-388 and the DNA binding mutant protein yTAF4 151-388Δ311-350 at 25°C (Fig. 7A), but there was no growth with the DNA binding mutant protein at 37°C. Expression of these two yTAF4 derivatives in the shuffled strain was verified by immunoblot analysis of extracts prepared from cells grown at 23°C (Fig. 7B). This result suggests that the temperature sensitivity is due to reduced DNA binding activity. To test the effect of the DNA binding mutation on overall RNA polymerase II transcription, we measured the levels of mRNA in yTAF4 151-388 and yTAF4 151-388Δ311-350 strains at 23°C and 2 h after a shift to 37°C. The mRNA level in the DNA binding mutant was lower than that in the yTAF4 151-

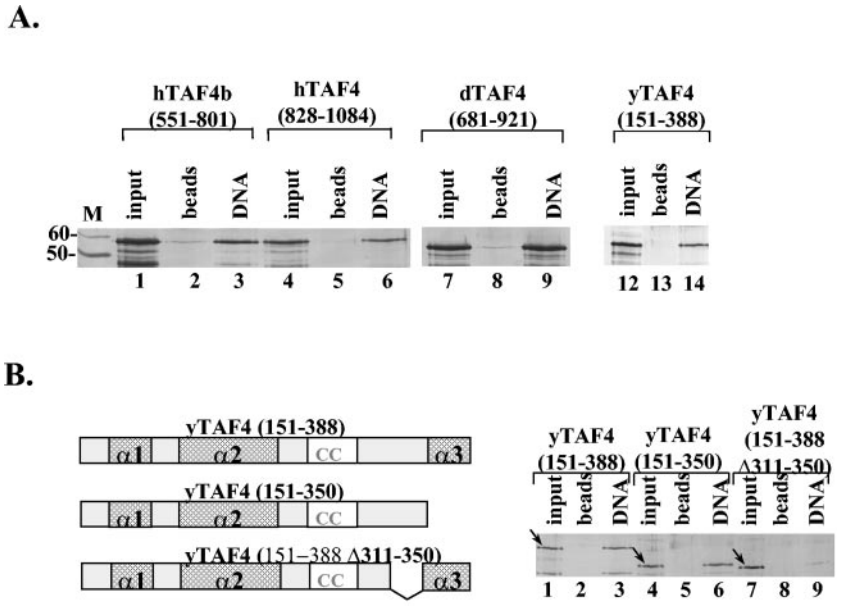

FIG. 6. DNA binding by TAF4 is evolutionarily conserved. (A) The C-terminal domains of the H2A-like hTAF4, dTAF4, and yTAF4 were cloned, expressed as GST fusion proteins, and analyzed for binding to DNA-cellulose (DNA) or cellulose beads (beads). Twenty percent of the eluted proteins was analyzed by SDS-PAGE, followed by silver staining. The identity of the proteins was verified by immunoblotting with GST-specific antibodies (data not shown). (B) Analysis of DNA binding mutant derivatives of yTAF4. Mutant derivatives of the yTAF4 protein corresponding to hTAF4b 551–769 and 551–801Δ735–769 (Fig. 5) were constructed as GST fusion proteins and analyzed for DNA binding activity with DNA-cellulose (DNA) or empty cellulose beads (beads). The mutant proteins, shown schematically at the left, have either the third α-helix or part of the spacer domain deleted, as indicated above the lanes.

388 mutant at both temperatures (Fig. 7C). These results suggest that TAF4 DNA binding is important for transcription.

DNA binding by hTAF4b-hTAF12 complex. Genetic studies with yeast (30) and immunocolocalization experiments with TFIID, as visualized by electron microscopy (20), provided strong evidence that the hTAF4-hTAF12 complex exists not only in vitro but also in the native TFIID. Therefore we analyzed TAF12 for binding to DNA-cellulose and found that it can also bind DNA (Fig. 8A, lanes 13 to 15). To test whether the HFD-mediated interaction between TAF4b and TAF12 plays a role in DNA binding, we used DNA-cellulose binding and EMSAs (Fig. 8A and B, respectively). The results show good correlation between the amounts of hTAF12 and TAF4b bound to the DNA-cellulose, suggesting that association of TAF4b with hTAF12 neither inhibited nor enhanced the amount of the DNA-bound proteins. In the EMSA experiments the TAF12 DNA-protein complex is not stable enough to withstand electrophoresis and is not detected (Fig. 8B, lane 3) whereas the TAF4b DNA-protein complex is clearly detected but seems to dissociate during the electrophoresis, as indicated by the extended appearance of the protein-DNA band (lane 2). Strikingly, a complex composed of both TAF4b and TAF12 displays significantly less dissociation during electrophoresis, suggesting that TAF4-TAF12 forms a more stable complex with DNA than TAF4b alone. Densitometric measurement of the bound DNA indicates that the same amount of DNA is bound by TAF4b alone and TAF4b-TAF12 (Fig. 8B, bottom). Analysis of the TAF4b-TAF12 complex by gel filtration suggests that it is a tetramer (our unpublished data). Thus, while the HFD-mediated TAF4b-TAF12 interaction does not affect the protein-DNA complex quantitatively, it contributes significantly to its stability.

DNA binding by a histone-like TAF octamer composed of TAF6-TAF9 and TAF4b-TAF12. A previous study suggested that yTAF6 and yTAF9 (H3-H4-like TAFs) form a histone octamer-like complex with yTAF4 and yTAF12 (H2A-H2B-like) in vitro. As with histones, formation of the TAF octameric complex is mediated by their HFDs, but unlike the histones, this complex was reported to lack DNA binding activity (30). Given that TAF6-TAF9 displays sequence-specific binding, we considered that in a histone-like octamer the specificity could be directed by TAF6-TAF9 while TAF4b-TAF12 could contribute to the complex additional contacts with the DNA, with both effects facilitating core promoter binding. To test this possibility, we reconstituted a putative octamer-like complex by incubating similar amounts of preformed TAF6-TAF9 and TAF4b-TAF12 complexes. Formation of a complex between TAF6-TAF9 and TAF4b-TAF12 was confirmed by coimmunoprecipitation experiments with TAF9- and TAF12-specific antibodies directed against each of the pairs (Fig. 9A). As in each of the pairs the stoichiometry is ~1:1, and the ratios between the pairs in the input and the immunoprecipitated proteins are similar, the complex formed between the pairs is likely to have a stoichiometry close to 1:1. We compared the DNA binding activity of this putative TAF octameric complex to the activity of each of the pairs using suboptimal amounts of each of the pairs. As shown in Fig. 9B, both TAF6-TAF9 and TAF4b-TAF12 pairs formed a DNA-protein complex which tends to dissociate during electrophoresis, as evident from the significant amount of retarded smear. Remarkably, upon mix-

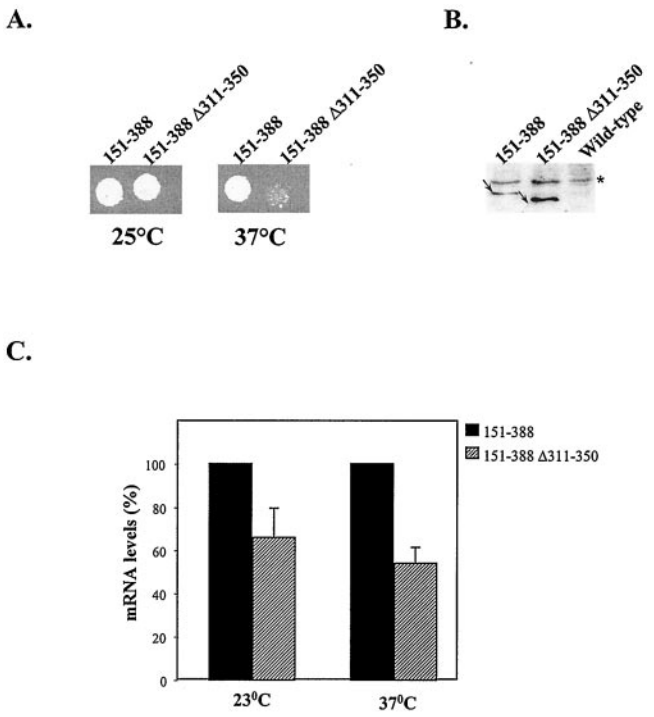

FIG. 7. (A) TAF4 DNA binding mutation confers temperature-sensitive growth and reduces mRNA transcription. A yTAF4 null strain carrying plasmids expressing either yTAF4 hemagglutinin (HA)-151-388 or yTAF4 HA-151-388Δ311-350 was grown on plates at 25 and 37°C. (B) Immunoblot analysis using an anti-HA antibody of cell extract prepared from a TAF4 null yeast strain that bears the coding sequence for wild-type TAF4 on a plasmid (wild type) or from the same cells transformed with yTAF4 HA-151-388 or yTAF4 HA-151-388Δ311-350, with the wild-type TAF4 plasmid shuffled out. Arrows, HA-TAF4 derivatives; asterisk, nonspecific protein that cross-reacts with the HA antibody. (C) Comparison of the total mRNA levels at 23°C and after a 2-h shift to 37°C between yeast strains carrying yTAF4 151-388 and yTAF4 151-388Δ311-350. The mRNA level of yTAF4 151-388 strain was set to 100%. The results presented are averages of two independent experiments.

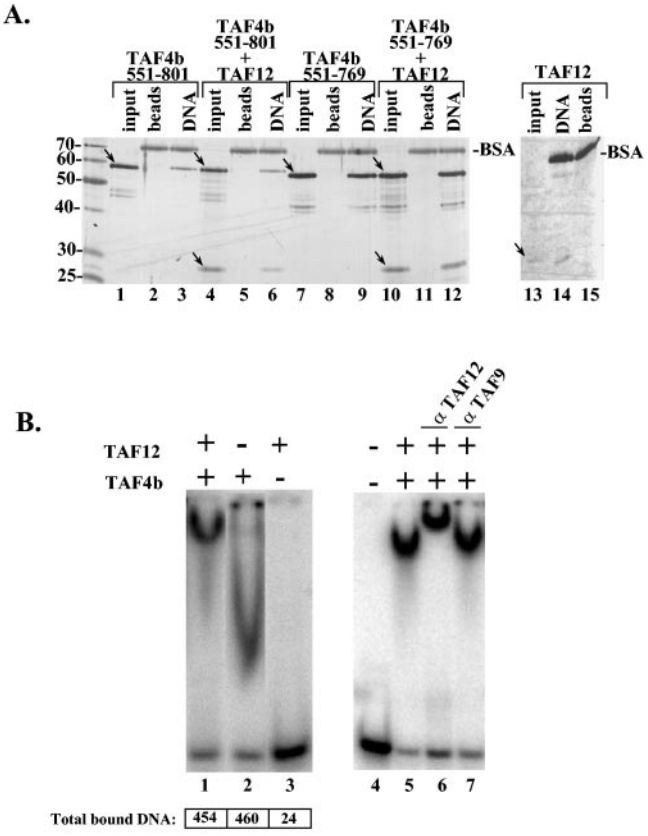

FIG. 8. Interaction of TAF4b with TAF12 increases the stability but not the quantity of the DNA-bound complex. (A) Analysis of the binding of TAF4b 551–801 and TAF4b 551–769 to DNA-cellulose or to empty cellulose beads in the presence or absence of hTAF12 (lanes 1 to 12). The binding of TAF12 alone is shown in lanes 13 to 15. The bound proteins were eluted by high salt, and 20% of the eluted proteins was analyzed by SDS-PAGE and silver staining. The position of BSA, present in the binding buffer, is indicated. The proteins used for binding are shown at the top. Arrows, positions of hTAF4b and hTAF12. (B) Analysis of the DNA binding of equal amounts of purified TAF4b and TAF12 proteins, either alone or as a complex, by EMSA. The probe used is the J-chain core promoter. The amounts of bound DNA were quantified and are presented as densitometric units (bottom left). (Right) The protein-DNA complex was preincubated with either a TAF12-specific antibody or TAF9-specific antibodies, which serve as a negative control.

ing TAF6-TAF9 with TAF4b-TAF12 to give an approximate ratio of 1:1 between the pairs, the complex composed of the four TAFs binds more DNA than the sum of the pairs, and the putative octamer-DNA complex is significantly more stable than each pair alone, as there is relatively less retarded smear in the octameric complex (see the densitometric measurement of the bound DNA in Fig. 9B, bottom). There are approximately six- and threefold increases in the ratio between the amounts of stable and unstable DNA-protein complex in the putative octamer-DNA complex relative to the corresponding amounts for TAF9-TAF6 and TAF4b-TAF12, respectively. It is possible that the additional points of contacts provided by TAF4-TAF12 to the DNA and to TAF6-TAF9 proteins increase its resistance to the electric field in the EMSA.

To confirm that the DNA-protein complex detected upon mixing of TAF6-TAF9 with TAF4b-TAF12 is indeed composed of each of these pairs, we added specific antibodies to the DNA binding reaction: anti-TAF9 polyclonal antibodies for the TAF6-TAF9 pair and an anti-TAF12 monoclonal antibody for the TAF4-TAF12 pair. The anti-TAF1 monoclonal antibody served as a specificity control. Increasing amounts of TAF9 antibodies inhibited the formation of the protein-DNA complex of the putative octamer (compare lanes 2 and 3 to lane 1 in Fig. 9C). The effect is specific, as these antibodies similarly inhibited the TAF6-TAF9–DNA complex alone (Fig. 2C) but had no effect on the TAF4b-TAF12–DNA complex (Fig. 8B). The TAF12 antibody also affected the putative octamer-DNA complex by reducing its mobility (Fig. 9C, compare lane 4 to 1), while the TAF1 antibody was without effect (lane 5). The specificity of the TAF12 antibody was checked on the TAF6-TAF9 DNA-protein complex and had no effect (Fig. 2C), while it clearly supershifted the TAF4b-TAF12–DNA complex (Fig. 8B). The effect of both TAF9 and TAF12 antibodies on the entire DNA-bound complex provides additional evidence that the octamer-like complex is composed of stoichiometric amounts of each of the pairs. We also tested the

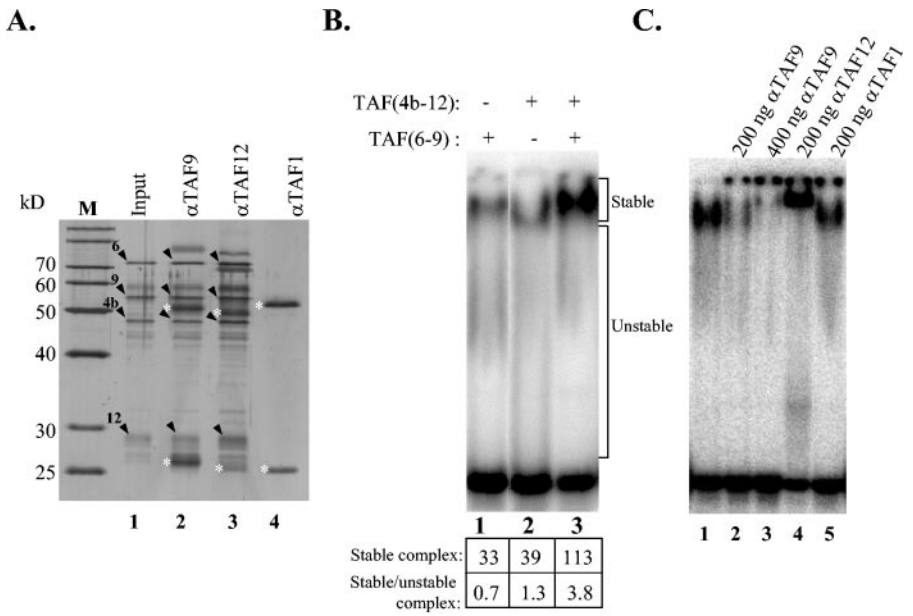

FIG. 9. DNA binding by the putative histone-like TAF octamer. (A) The purified TAF6-TAF9 complex was mixed with the purified TAF4b-TAF12 complex for 30 min and then subjected to coimmunoprecipitation using antibodies specific to each pair: TAF9-specific polyclonal antibodies, a TAF12 monoclonal antibody, and a TAF1 antibody as a negative control. The input and the immunoprecipitated proteins were analyzed by SDS-PAGE and silver staining. Arrowheads, positions of the TAFs; asterisks, positions of the immunoglobulin heavy and light chains. (B) The purified TAF6-TAF9 complex was incubated with the purified TAF4b-TAF12 complex for 30 min and then subjected to a DNA binding reaction with the IRF-1 core promoter probe (lane 3). Binding reactions involving the same amounts of TAF6-TAF9 and TAF4b-TAF12 alone, as indicated at the top, are shown in lanes 1 and 2. The bound DNA was quantified, and levels are presented as densitometric units at the bottom. The ratio of stable to unstable (smeared) DNA-protein complex for each binding reaction was also quantified as shown. (C) Analysis of the putative octameric complex by antibodies. The indicated antibodies (top) were preincubated with the putative TAF-octamer complex and then used for a DNA binding assay.

sequence specificity of the putative histone-like TAF octamer by competition experiments and found that the preference for DPE is retained (data not shown). Together these results suggest that hTAF6-hTAF9 forms a histone-like octamer with TAF4b-TAF12 which binds the DPE-containing core promoter more efficiently and stably than TAF6-TAF9 alone.

DISCUSSION

Of the 14 subunits of TFIID, 9 contain a histone fold motif, a well-characterized protein-protein interaction domain. In the present study we assign novel and important functions to the HFD and also to other highly conserved and essential domains of the four TAFs that we investigated. These domains, HFD and non-HFD together, form an octamer-like unit in TFIID, which binds DNA specifically and with great stability and thus may be critical to TFIID's major function of core promoter recognition and binding. We provide evidence for three different ways by which the histone fold motifs contribute to core promoter binding. First, HFD-mediated protein-protein interaction enhances and stabilizes the interaction of the TAFs with DNA. Second, the HFD-mediated association is critical for sequence-specific binding. Third, the HFD of one TAF (TAF4b) mediates direct contacts with DNA.

Core promoter binding by the H3-H4-like TAF9 and TAF6. Previous studies showed that TAF9 and TAF6 are likely to bind DNA (5); however, neither the mode by which these two TAFs bind to DNA nor the importance of their HFDs for this activity was known. Our study revealed that these TAFs have intrinsic DNA binding activity that lies outside the HFD. Nevertheless the interaction of these TAFs through the HFD dramatically enhanced the DNA binding activity and was critical for the specificity for the core promoter motif DPE.

The functional importance of DPE as a core promoter element was nicely demonstrated in *Drosophila* (5, 6) and in vertebrates (9). Our study extends these observations by providing the molecular basis for the association of TAF9 with DPE-containing promoters. We found that the DNA binding activity exerted by the essential CR domain of TAF9 (8) is linked to the HFD by virtue of interaction with TAF6 via its HFD.

Role of the unique HFD of TAF4 and HFD-dependent interaction with TAF12. We demonstrate for the first time that TAF4 has significant DNA binding activity. It was observed in the context of the TFIID complex, and in the isolated protein, it is preserved throughout evolution from yeast to humans and is required for transcription of some yeast genes, suggesting that it has an important function.

TAF4 family members have an atypical histone fold motif with a long spacer between the second and the third helices. TAF4b DNA binding appears to require the H2A-like histone fold structural motif and part of the unique spacer domain. However, unlike H2A, which contacts DNA through the first α-helix and the two loops of the histone fold domain (21), TAF4b DNA binding is mediated by the second α-helix. This is a fundamental difference in the mode of DNA binding between TAF4 and histone H2A and explains why the DNA-contacting residues in H2A were not preserved in the TAF4

family. In addition to its direct DNA binding, TAF4b HFD interacts with the H2B-like TAF12, and this interaction increases the stability of the complex with the DNA. The importance of the spacer domain is evolutionarily conserved, as its deletion from both hTAF4b and yTAF4 significantly reduced DNA binding and impaired transcription of some yeast genes.

Our results seemingly contradict a recent structural characterization of the hTAF4-hTAF12 heterodimeric complex that led the authors to suggest that the hTAF4-hTAF12 histone-like pair is unlikely to bind DNA (36). Their assumption was that DNA binding by hTAF4-hTAF12 is mediated by charge-like histones. Two observations can explain the apparent incompatibility with our findings. First, the mode of TAF4b DNA binding is different from that of histone H2A and therefore may be less dependent on charge. Second, hTAF4 in the reported structural analysis consisted of only the first and second helices of the histone fold but was without the unique spacer domain that is essential for DNA binding.

The potential of TAF4 to contact DNA was noted in UV cross-linking studies (24). However, these experiments could not distinguish between TAFs that have identical mobility by SDS-PAGE, such as hTAF2 and hTAF4, or between TAFs that directly contact the DNA and those in close proximity due to the long arm of the cross-linker.

DNA binding by the histone-like TAF octamer within TFIID. The H3-H4-like module in TAF6-TAF9 HFD interacts with the H2A-H2B-like TAF4-TAF12 to form a histone-like octamer complex. We show that such an octameric complex binds DNA with greater efficiency and stability than the individual pairs. If such a histone-like octamer does exist within TFIID, as genetic studies imply (30), it is likely to facilitate TFIID interaction with DNA. The DNA binding associated with the four TAFs examined here suggests that other TAFs with or without HFDs may also contribute to core promoter binding. Analysis of the rest of the TAFs for DNA binding is likely to broaden our understanding of the mechanisms by which TFIID interacts with the large repertoire of core promoter sequences that exist in the genomes of the higher eukaryotes.

ACKNOWLEDGMENTS

We thank P. Anthony Weil for the TAF4 null yeast strain, Irwin Davidson for the TAF12 antibody, Laszlo Tora for the TAF6 antibody, Arthur Liberzon for indicating to us the temperature sensitivity phenotype of the yTAF4 151–388Δ311–350 strain, and R. Tjian and Elena Ainbinder for their comments on parts of the manuscript.

This work was supported by grants from the Israel Science Foundation, the Woman Health Research Center of the Weizmann Institute of Science, and the Minerva Foundation of Germany. R.D. is an incumbent of the Martha S. Sagon Career Development Chair.

REFERENCES

1. **Ainbinder, E., M. Revach, O. Wolstein, S. Moshonov, and R. Dikstein.** 2002. The mechanism of rapid transcriptional induction of tumor necrosis factor alpha-responsive genes by NF-κB. Mol. Cell. Biol. **22:**6354–6362.
2. **Albright, S. R., and R. Tjian.** 2000. TAFs revisited: more data reveal new twists and confirm old ideas. Gene **242:**1–13.
3. **Brand, M., K. Yamamoto, A. Staub, and L. Tora.** 1999. Identification of TATA-binding protein-free TAFII-containing complex subunits suggests a role in nucleosome acetylation and signal transduction. J. Biol. Chem. **274:** 18285–18289.
4. **Breiling, A., B. M. Turner, M. E. Bianchi, and V. Orlando.** 2001. General transcription factors bind promoters repressed by Polycomb group proteins. Nature **412:**651–655.
5. **Burke, T. W., and J. T. Kadonaga.** 1997. The downstream core promoter element, DPE, is conserved from *Drosophila* to humans and is recognized by TAFII60 of *Drosophila*. Genes Dev. **11:**3020–3031.
6. **Butler, J. E., and J. T. Kadonaga.** 2001. Enhancer-promoter specificity mediated by DPE or TATA core promoter motifs. Genes Dev. **15:**2515–2519.
7. **Chalkley, G. E., and C. P. Verrijzer.** 1999. DNA binding site selection by RNA polymerase II TAFs: a TAF(II)250-TAF(II)150 complex recognizes the initiator. EMBO J. **18:**4835–4845.
8. **Chen, Z., and J. L. Manley.** 2003. In vivo functional analysis of the histone 3-like TAF9 and a TAF9-related factor, TAF9L. J. Biol. Chem. **278:**35172–35183.
9. **Chen, Z., and J. L. Manley.** 2003. Core promoter elements and TATA box-binding protein-associated factors contribute to the diversity of transcriptional activation in vertebrates. Mol. Cell. Biol. **23:**7350–7362.
10. **Dikstein, R., S. Zhou, and R. Tjian.** 1996. Human TAFII105 is a cell type specific TFIID subunit related to hTAFII130. Cell **87:**137–146.
11. **Emanuel, P. A., and D. S. Gilmour.** 1993. Transcription factor TFIID recognizes DNA sequences downstream of the TATA element in the hsp70 heat shock gene. Proc. Natl. Acad. Sci. USA **90:**8449–8453.
12. **Freiman, R. N., S. R. Albright, S. Zheng, W. C. Sha, R. E. Hammer, and R. Tjian.** 2001. Requirement of tissue-selective TBP-associated factor TAFII105 in ovarian development. Science **293:**2084–2087.
13. **Gangloff, Y. G., C. Romier, S. Thuault, S. Werten, and I. Davidson.** 2001. The histone fold is a key structural motif of transcription factor TFIID. Trends Biochem. Sci. **26:**250–257.
14. **Gangloff, Y. G., S. Werten, C. Romier, L. Carre, O. Poch, D. Moras, and I. Davidson.** 2000. The human TFIID components $TAF_{II}135$ and $TAF_{II}20$ and the yeast SAGA components ADA1 and $TAF_{II}68$ heterodimerize to form histone-like pairs. Mol. Cell. Biol. **20:**340–351.
15. **Grant, P. A., D. Schieltz, M. G. Pray-Grant, D. J. Steger, J. C. Reese, J. R. Yates III, and J. L. Workman.** 1998. A subset of TAF(II)s are integral components of the SAGA complex required for nucleosome acetylation and transcriptional stimulation. Cell **94:**45–53.
16. **Guermah, M., Y. Tao, and R. G. Roeder.** 2001. Positive and negative TAF_{II} functions that suggest a dynamic TFIID structure and elicit synergy with TRAPs in activator-induced transcription. Mol. Cell. Biol. **21:**6882–6894.
17. **Hoffmann, A., C. M. Chiang, T. Oelgeschlager, X. Xie, S. K. Burley, Y. Nakatani, and R. G. Roeder.** 1996. A histone octamer-like structure within TFIID. Nature **380:**356–359.
18. **Hoffmann, A., T. Oelgeschläger, and R. G. Roeder.** 1997. Considerations of transcriptional control mechanisms: do TFIID-core promoter complexes recapitulate nucleosome-like functions? Proc. Natl. Acad. Sci. USA **94:**8928–8935.
19. **Kaufmann, J., and S. Smale.** 1994. Direct recognition of initiator elements by a component of the transcription factor IID complex. Genes Dev. **8:**821–829.
20. **Leurent, C., S. Sanders, C. Ruhlmann, V. Mallouh, P. A. Weil, D. B. Kirschner, L. Tora, and P. Schultz.** 2002. Mapping histone fold TAFs within yeast TFIID. EMBO J. **21:**3424–3433.
21. **Luger, K., A. W. Mader, R. K. Richmond, D. F. Sargent, and T. J. Richmond.** 1997. Crystal structure of the nucleosome core particle at 2.8 Å resolution. Nature **389:**251–260.
22. **Martinez, E., T. K. Kundu, J. Fu, and R. G. Roeder.** 1998. A human SPT3-TAFII31-GCN5-L acetylase complex distinct from transcription factor IID. J. Biol. Chem. **273:**23781–23785.
23. **Nakatani, Y., M. Horikoshi, M. Brenner, T. Yamamoto, F. Bresnard, R. G. Roeder, and E. Freese.** 1990. A downstream initiation element required for efficient TATA box-binding and in vitro function of TFIID. Nature **348:**86–88.
24. **Oelgeschlager, T., C. M. Chiang, and R. G. Roeder.** 1996. Topology and reorganization of a human TFIID-promoter complex. Nature **382:**735–738.
25. **Ogryzko, V. V., T. Kotani, X. Zhang, R. L. Schiltz, T. Howard, X. J. Yang, B. H. Howard, J. Qin, and Y. Nakatani.** 1998. Histone-like TAFs within the PCAF histone acetylase complex. Cell **94:**35–44.
26. **Purnell, B. A., P. A. Emanuel, and D. S. Gilmour.** 1994. TFIID sequence recognition of the initiator and sequences farther downstream in *Drosophila* class II genes. Genes Dev. **8:**830–842.
27. **Sanders, S. L., and P. A. Weil.** 2000. Identification of two novel TAF subunits of the yeast *Saccharomyces cerevisiae* TFIID complex. J. Biol. Chem. **275:** 13895–13900.
28. **Saurin, A. J., Z. Shao, H. Erdjument-Bromage, P. Tempst, and R. E. Kingston.** 2001. A *Drosophila* Polycomb group complex includes Zeste and dTAFII proteins. Nature **412:**655–660.
29. **Sawadogo, M., and R. G. Roeder.** 1985. Interaction of a gene-specific transcription factor with the adenovirus major late promoter upstream of the TATA box region. Cell **43:**165–175.
30. **Selleck, W., R. Howley, Q. Fang, V. Podolny, M. G. Fried, S. Buratowski, and S. Tan.** 2001. A histone fold TAF octamer within the yeast TFIID transcriptional coactivator. Nat. Struct. Biol. **8:**695–700.
31. **Silkov, A., O. Wolstein, I. Shachar, and R. Dikstein.** 2002. Enhanced apoptosis of B and T lymphocytes in $TAF_{II}105$ dominant negative transgenic mice is linked to NF-κB. J. Biol. Chem. **277:**17281–17829.
32. **Thuault, S., Y. G. Gangloff, J. Kirchner, S. Sanders, S. Werten, C. Romier, P. A. Weil, and I. Davidson.** 2002. Functional analysis of the TFIID-specific

yeast TAF4 (yTAFII48) reveals an unexpected organisation of its histone fold domain. J. Biol. Chem. **277:**45510–45517.
33. **Verrijzer, C. P., J. L. Chen, K. Yokomori, and R. Tjian.** 1995. Binding of TAFs to core elements directs promoter selectivity by RNA polymerase II. Cell **81:**1115–1125.
34. **Verrijzer, C. P., K. Yokomori, J. L. Chen, and R. Tjian.** 1994. *Drosophila* TAFII150: similarity to yeast gene TSM-1 and specific binding to core promoter DNA. Science **264:**933–941.
35. **Wang, J. C., and M. W. Van Dyke.** 1993. Initiator sequences direct downstream promoter binding by human transcription factor IID. Biochim. Biophys. Acta **1216:**73–80.
36. **Werten, S., A. Mitschler, C. Romier, Y. G. Gangloff, S. Thuault, I. Davidson, and D. Moras.** 2002. Crystal structure of a subcomplex of human TFIID formed by TBP-associated factors hTAF4 (hTAFII135) and hTAF12 (hTAFII20). J. Biol. Chem. **277:**45502–45509.
37. **Wolstein, O., A. Silkov, M. Revach, and R. Dikstein.** 2000. Specific interaction of TAFII105 with OCA-B is involved in activation of octamer-dependent transcription. J. Biol. Chem. **275:**16459–16465.
38. **Xie, X., T. Kokubo, S. L. Cohen, U. A. Mirza, A. Hoffmann, B. T. Chait, R. G. Roeder, Y. Nakatani, and S. K. Burley.** 1996. Structural similarity between TAFs and the heterotetrameric core of the histone octamer. Nature **380:** 316–322.
39. **Yamit-Hezi, A., and R. Dikstein.** 1998. $TAF_{II}105$ mediates activation of anti-apoptotic genes by NF-κB. EMBO J. **17:**5161–5169.